

PNL-SA--20784

DE93 008260

SOFC CHROMITE SINTERING AND
ELECTROLYTE/AIR-ELECTRODE
INTERFACE REACTIONS

DISCLAIMER

This report was prepared as an account of work sponsored by an agency of the United States Government. Neither the United States Government nor any agency thereof, nor any of their employees, makes any warranty, express or implied, or assumes any legal liability or responsibility for the accuracy, completeness, or usefulness of any information, apparatus, product, or process disclosed, or represents that its use would not infringe privately owned rights. Reference herein to any specific commercial product, process, or service by trade name, trademark, manufacturer, or otherwise does not necessarily constitute or imply its endorsement, recommendation, or favoring by the United States Government or any agency thereof. The views and opinions of authors expressed herein do not necessarily state or reflect those of the United States Government or any agency thereof.

J. L. Bates
L. A. Chick
G. E. Youngblood

April 1992

Presented at the
Workshop of Fuel Cell Technology
Research and Development
April 29-30, 1992
San Francisco, California

RECEIVED
FEB 23 1993
OSTI

Prepared for
the U.S. Department of Energy
under Contract DE-AC06-76RLO 1830

Pacific Northwest Laboratory
Richland, Washington 99352

MASTER

DISTRIBUTION OF THIS DOCUMENT IS UNLIMITED

SP

SOFC CHROMITE SINTERING AND ELECTROLYTE/AIR-ELECTRODE INTERFACE REACTIONS

J. L. Bates, L.A. Chick and G.E. Youngblood
Pacific Northwest Laboratory^a
P.O. Box 999
Richland, Washington 99352

PNL-SA--20784
DE93 008260

CHROMITE SINTERING

Introduction

The air sintering behaviors of chromites has been investigated in three systems, La(Sr)CrO₃ (LSC), La(Ca)CrO₃ (LCC), and Y(Ca)CrO₃ (YCC). This presentation will discuss the effects of alkaline earth concentration and chromium enrichment or depletion on chromite sintered densities and microstructures. Liquid-phase sintering appears dominant in YCC and LCC especially with Cr enrichment. Either vapor- or solid-phase transport may dominate in the LSC system. Slight depletion or enrichment of Cr has dramatic effects on air-sintered density and microstructure.

Experimental

Chromite powders were prepared by glycine/nitrate combustion synthesis [1-2]. The resulting powders were uniaxially pressed at 35 MPa and then isostatically pressed at 140 MPa and then sintered in stagnant or flowing (0.25 l/s) air in an electrically heated furnace.

Alkaline Earth Dopant Level Effects

Sintered densities generally increase as alkaline earth dopant level is increased up to about 25% substitution. For sintering at 1550°C for 8 hours, maximum relative densities were attained in flowing air for YCC containing Ca=0.20 (98% TD) and for LSC with Sr=0.24 (93% TD).

Shrinkage during sintering was determined for pellets by heating in a vertical pushrod dilatometer at 100°C/hr. YCC and LCC samples with $x > 0.12$ sintered rapidly between 1000 and 1100°C, with shrinkage proportional to calcium concentration. XRD indicates part of the Ca or Sr is exsolved as CaCrO₄ or SrCrO₄. These chromate compounds (or their solid decomposition products) melt near 1020°C for the YCC and LCC systems and near 1250°C for the LSC system. Near the maximum sintering temperature, the alkaline earths are again substituted into the perovskite phase. Thus, these chromites produce a transient sintering aid, although remnants of the liquid have been detected in some samples.

In Y_{0.6}Ca_{0.4}CrO₃ the progress of liquid-phase sintering can be readily detected in optical micrographs of polished sections. Samples were heated at 300°/hr to the desired temperature and quickly removed from the furnace. At 1100°C, the microstructure contains dense, irregular areas that are apparently formed by localized liquid-phase sintering. The dense masses grow and coalesce on further sintering above 1100°C. Finally, at 1550°C, the voids have coalesced into irregularly shaped pores. Further heating at 1550°C for 8 hours removes the smallest pores.

A series of LSC samples shows no discernable patterns of non-uniform densification as seen in the YCC samples. Rather, scanning electron microscopy (SEM) reveals grain growth in the LSC, from about 20 nm at room

^a Operated by Battelle Memorial Institute for the U.S. Department of Energy under Contract DE-AC06-76RLO 1830

temperature to about 500 nm by 1550°C. Therefore, although SrCrO₄ formation and subsequent melting at near 1250°C have been confirmed in LSC by high temperature XRD, the resulting liquid phase is apparently not as effective in causing densification as that in YCC. This implies that either grain boundary or bulk diffusion may account for densification of LSC, whereas vapor-phase transport probably accounts for much of the grain growth, as will be discussed.

Effects of Chromium Enrichment or Depletion

The effects of Cr depletion or enrichment were studied for LSC, YCC, and LCC compositions with alkaline earth substitution near 30%. For all three chromite systems, the highest densities were obtained for Cr depletion. Small depletions in Cr result in large changes in sintered morphology with a fully dense surface layer (100 to 200 μm) and an inhomogeneous, low-density interior. Energy dispersive spectroscopy analyses show that YCC samples with enriched Cr contain Cr-rich phase near the surface and, for larger Cr enrichments, within the interior. Cr-depleted samples exhibit a Ca-rich liquid-phase remnant near the surface and within the higher-density regions of the interior. LSC samples with Cr depletion sinter to high density but contain large crystals of La₂O₃, a phase susceptible to hydration, which causes cracking of the material.

The experimental evidence suggests that the alteration of the A/B cation ratio causes secondary phase formation in both the Ca- and Sr-containing systems. Meadowcroft and Wimmer [3] showed that enriched Cr in LSC resulted in greatly enhanced volatility of Cr oxides. For LSC and YCC, the role of vapor-phase transport can be complicated by secondary phase formation. The formation of the volatile Cr oxides, CrO₂ and CrO₃, and the formation of the liquid-phase-forming chromates, SrCrO₄ and CaCrO₄, both require access to oxygen. Therefore, possible detrimental effects of vapor phase transport can be offset by liquid-phase sintering resulting from chromate formation and melting.

In summary, although the roles of vapor-, liquid- and solid-phase transport in the chromites and their combined effects on densification are not yet fully understood, liquid-phase sintering appears more pronounced for Ca-containing chromites than for those that contain Sr. The absence of an obvious liquid phase in LSC indicates that solid-phase sintering, involving either bulk or grain boundary diffusion, may be the predominating densification mechanism. Therefore, LSC sintering appears to be dependent on the relative significance of vapor-phase versus solid-phase transport.

ELECTROLYTE/AIR-ELECTRODE INTERFACE REACTIONS

Introduction

The performance of high-temperature solid electrolyte cells is dependent upon the electrochemical processes that occur at solid-solid-gas interfaces. The SOFC processes involve a number of such interfaces, particularly those between the electrodes, electrolyte and gases. Changes in the character of the solid-solid interfaces representative of those for SOFC, can alter reactions mechanisms and reaction kinetics. The purpose of this research is to understand the roles that material composition, properties and structures, electric current and potential, temperature, environment and time exert upon these electrochemical interface processes. Such understanding can lead to improved materials, better cell fabrication and higher performance for SOFCs. This research emphasizes air-electrode/electrolyte interfaces with La_{1-x}Sr_xMnO₃ (LSM) electrodes. The roles of manganite properties, particularly mixed ionic-electronic conduction, is of special interest. To evaluate these factors requires a reproducible cell design that is independent of fabrication variables.

Experimental Procedures

Ac impedance spectroscopy and dc polarization techniques coupled with an unbonded interface cell (UIC) were used to study electrochemical reactions and performance of solid-solid-gas interfaces relating to SOFCs without the influences of interface morphology variations resulting from cell fabrication. The UIC utilized separately

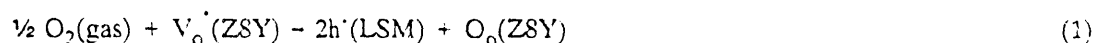
fabricated electrodes and electrolytes. Ground surfaces were placed in contact by spring loading, with the O₂-Ar gas permeating between the contacting, but unbonded surfaces. Only a small fraction of the surfaces were in contact. The contact area and solid-solid-gas triple point were calculated from the data.

The electrochemical cells, both half and symmetric, consisted of an 8 m/o Y₂O₃ stabilized ZrO₂ (ZSY) electrolyte with electrode materials of Pt bead (1) and Pt disc (2) for references, state-of-the-art La_{0.6}Sr_{0.1}MnO₃ (3), La_{0.7}Sr_{0.3}MnO₃ (4,5) and 0.2Y₂O₃-0.39PrO₂-0.39HfO₂-0.01Y₂O₃ (IPHY) (6). IPHY is a mixed ionic/electronic conductor. Complex impedance and dc polarization measurements were made from 600 to 1000° C at oxygen partial pressures from 0.00002 to 0.93 atm.

Complex impedance dispersion curves (Nyquist plots) obtained under isobaric and/or isothermal conditions over a 0.1Hz to 100 kHz range were analyzed using equivalent circuits. These circuits consisted of series and parallel combinations of resistances and capacitive-like constant phase elements. The bulk ohmic resistance (R_B) and dc polarization resistances (R_p) were extracted from fitting an equivalent circuit to the Nyquist plot. The effective reaction lengths (ERL), related to the triple phase boundary lengths, were obtained R_B using a model for non-uniform current distribution at a single-point interface. The values for R_p are inversely proportional to the cathodic reaction rate.

Air-Electrode/Electrolyte Reactions

The overall cathodic reaction for O₂ reduction at the LSM[†] electrolyte/ZSY electrolyte interface is:



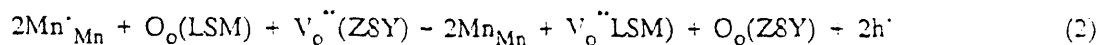
Enhanced electrocatalytic activity, which apparently occurs at the Mn³⁺ reaction sites in the LSM, is related to enhanced electronic conductivity in the LSM. It also appears that cathodic reaction rates are enhanced by increased oxygen-ion transport in LSM which results in an increased effective reaction area or ERL value. Of special interest are composition and electrochemical effects that can enhance the cathodic reaction rate.

Results and Discussion

The resistance, R_B, decreases with increasing temperature with T/R_B v.s. 1/T being linear. Activation energies vary from 0.71 eV (IPHY) and between 0.91 and 1.14 eV for all others. These latter values bracket the 0.95 eV for ZSY. This general agreement for cathodic materials suggests that single-point and multiple point contacts are equivalent. The R_B are also independent of P(O₂) between 0.00002 and 0.93 atm, except for La_{0.7}Sr_{0.3}MnO₃, sample 4 and 5. The ERL values for Pt and La_{0.9}Sr_{0.1}MnO₃ are relatively insensitive to changes in temperature and P(O₂), however, ERL for La_{0.7}Sr_{0.3}MnO₃ increase with decreasing P(O₂).

The dc polarization (R_p) at 1173 K in air varied significantly for electrodes of Pt(bead) and La_{1-x}Sr_xMnO_{3±y} with x = 0.1 and 0.3. The higher cathodic potentials reflect different catalytic activities with LSM (x=0.1) < Pt < LSM (x=0.3). For La_{0.7}Sr_{0.3}MnO₃, a critical cathodic bias (E_c) occurs with a abrupt increase in current near -100 mV. Only a small critical bias change is observed at -200 mV for La_{0.9}Sr_{0.1}MnO₃.

The effective reaction area and therefore the electrochemical activity can also be increased by short application of a higher negative potential. This is attributed to increased concentration of V_o^{••} and h[•] at the surface of the LSM. The above is consistent with a proposed reaction mechanism suggesting that a cathodic current flowing through the cell partially reduces the electrode material near the electrolyte via the reaction:



for E_c > -100 mV for x = 0.3.

Conclusions

- Ac impedance spectroscopy and dc polarization techniques coupled with an unbonded interface cell were used to examine SOFC electrochemical reactions at solid-solid-gas interfaces. The electrochemical performance of $\text{La}_{1-x}\text{Sr}_x\text{MnO}_3$ ($x = 0.1$ and 0.3) and Pt bead air electrodes/ $(\text{Y}_2\text{O}_3)\text{ZrO}_2$ interfaces were compared to that for Pt electrodes.
- The effective reaction length (area) in $\text{La}_{1-x}\text{Sr}_x\text{MnO}_3$ increases slightly with increasing temperature and can be modified electrochemically by applying an external potential.
- The reaction kinetics for an $\text{La}_{1-x}\text{Sr}_x\text{MnO}_3/(\text{Y}_2\text{O}_3)\text{ZrO}_2$ interface can be enhanced significantly by an applied potential exceeding an apparent critical value.
- The reaction kinetics for $\text{La}_{0.9}\text{Sr}_{0.1}\text{MnO}_3$ are less than that for Pt. The reaction kinetics for $\text{La}_{0.7}\text{Sr}_{0.3}\text{MnO}_3$ are significantly greater than that for Pt.
- The dissociation of the O_2 molecule into adsorbed O atoms near the effective reaction zone appear to limit the reaction kinetics at the $\text{La}_{0.9}\text{Sr}_{0.1}\text{MnO}_3/8\%\text{Y}_2\text{O}_3\text{-ZrO}_2$ interface.

REFERENCES

1. L.A. Chick, J.L. Bates, L.R. Pederson, and H.E. Kissinger. 1989. "Synthesis of Air-Sinterable Lanthanum Chromite Powders". Proc. First International Symposium: Solid Oxide Fuel Cells. Hollywood, FL. Subhash C. Singal, Ed. Electrochemical Society, Inc. Pennington, NJ. pp.170-187.
2. L.A. Chick, L.R. Pederson, G.D. Maupin, J.L. Bates, L.E. Thomas, and G.J. Exarhos. 1990. "Glycine-nitrate Combustion Synthesis of Oxide Ceramic Powders". Materials Letters **10** (1.2). pp. 6-12.
3. L.A. Chick, J.L. Bates and G.D. Maupin. 1991. "Air-Sintering Mechanisms of Chromites". Proceedings Second International Symposium on Solid Oxide Fuel Cells. F. Grosz, P. Zegers, S.C. Singhal and O. Yamamoto, Eds. EUR 13564. Athens Greece. Commission of the European Communities, Luxembourg. pp. 621-628.
4. D.B. Meadowcroft and J.M. Wimmer. 1979. "Oxidation and Vaporization Processes in Lanthanum Chromite". Amer. Ceram. Soc. Bull. **58**. no.6. pp. 610-615.
5. Hammouche, A., E. Sieber, M. Kleitz and A. Hammou. 1989. "Oxygen Reduction at the $\text{La}_{1-x}\text{Sr}_x\text{MnO}_3$ /Zirconia Electrode". Proc. First International Symposium on Solid Oxide Fuel Cells. Electrochemical Society, Inc. **89-11**. pp. 265-76.

END

**DATE
FILMED**

5 103 193

